Lab on a Chip

Cite this: *Lab Chip*, 2012, **12**, 1089

www.rsc.org/loc

PAPER

Microfluidic nanoplasmonic-enabled device for multiplex DNA detection†

Hsin-I Peng,[a] Christopher M. Strohsahl[b] and Benjamin L. Miller*[ab]

Received 15th November 2011, Accepted 11th January 2012
DOI: 10.1039/c2lc21114a

We describe a rapid, quantitative, multiplex, self-labelled, and real-time DNA biosensor employing Ag nanoparticle-bound DNA hairpin probes immobilized in a microfluidic channel. Capture of complementary target DNAs by the microarrayed DNA hairpin probes results in a positive fluorescence signal *via* a conformational change of the probe molecules, signalling the presence of target DNAs. The device's capability for quantitative analyses was evaluated and a detection time as low as 6 min (with a target flow rate of 0.5 μl min^{-1}) was sufficient to generate significant detection signals. This detection time translates to merely 3 μl of target solution consumption. An unoptimized sensitivity of 500 pM was demonstrated for this device.

Introduction

The past two decades have witnessed the rapidly growing use of microfluidic technology in numerous bio-analytical devices including bio-separations systems,[1] biosensors,[2–5] and on-chip Polymerase Chain Reaction (PCR)[6,7] devices. This shift has been driven by the unique set of advantages that microfluidics provides in the context of bio-analytical studies. The ability to perform operations in a micron scale naturally translates into low reagent and power consumption, low cost, and portability.[8–12] At the same time, the micron-size channel height guides analytes to the immediate proximity of the reaction surface very efficiently, thus minimizing diffusion-limit reactions. Moreover, convection flow can rapidly replenish depleted reactants near the reaction surface, thereby increasing the reaction kinetics and resulting in rapid analysis. These criteria, combined with their suitability for multiplex analysis and real-time monitoring,[13] make microfluidics-enabled devices particularly powerful.

In this paper, we describe the implementation of a metal-enhanced fluorescence[14] (MEF) enabled biosensor in a microfluidic format for multiplex, quantitative DNA detection. This work builds on an arrayable and self-labelled DNA detection system on a planar Au surface previously developed in our laboratory.[15–17] In the absence of target DNA, a fluorophore-labelled (3′) and metal surface-immobilized DNA probe folds itself into a hairpin structure, concomitantly placing its attached fluorophore in close proximity to the metal surface. This results in fluorescence quenching. When a complementary target DNA is present, hybridization to the surface-immobilized probe DNA unfolds the hairpin, in turn moving the fluorophore away from the metal surface, preventing quenching and thereby signalling the presence of the specific target DNA through a fluorescence intensity increase. When combined with methods for the identification of "natural" hairpin probes, this strategy can produce a sensor with exceptionally high selectivity.[18]

In subsequent work, we demonstrated that the ability of Ag nanoparticles to dramatically amplify signals *via* MEF could significantly enhance sensor performance[19] (Fig. 1). In response to identical amounts of target DNA, nanostructured Ag substrates provided post-hybridization sensor signals over 10-fold higher than the responses from planar Au films. As strong signals could be obtained from substrates functionalized at low Ag nanoparticle density, the transparent nature of these DNA chips (potentially allowing imaging either above the chip

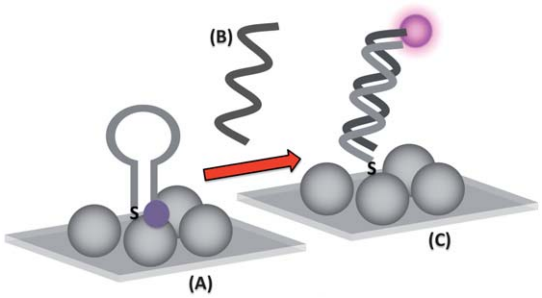

Fig. 1 Working principle of the plasmonic-enabled DNA biosensor. (A) An Ag surface-immobilized DNA probe folds itself into a hairpin structure in the absence of a target DNA. This in turn brings the probe-attached fluorophore in close proximity to the Ag surface and quenches the fluorescence due to energy transfer. (B) Addition of a complementary target DNA (C) hybridizes with the DNA hairpin probes, unwraps the DNA hairpin probe, and liberates the fluorophore from the quenching surface to the fluorescence enhancing zone nearby the Ag nanoparticles, signalling the presence of a specific DNA sequence.

[a]*Department of Biomedical Engineering, University of Rochester, Rochester, NY, 14627, USA*
[b]*Department of Dermatology, University of Rochester, Rochester, NY, 14627, USA*

† Electronic supplementary information (ESI) available: Additional fluorescence microarray images and discussion of probe design. See DOI: 10.1039/c2lc21114a

or through it with equal facility) was tailor-made for implementation in a simple microfluidic system (Fig. 2).

Experimental

Nanostructured Ag substrate fabrication

Nanostructured Ag substrates were fabricated by covalent attachment of Ag nanoparticles to thiolated glass substrates. Microscope glass slides (VWR, Cat. No. 48300-025) were first diced into individual chips with dimensions of 1.7 cm × 2.5 cm using a diamond scribe. These glass chips were cleaned by soaking them in piranha solution (sulfuric acid: hydrogen peroxide 3 : 1; Caution: piranha solution is caustic and reacts vigorously with organics) for 15 min. The glass chips were then rinsed with distilled, deionized (DDI) water, soaked in a 10 M NaOH solution for 5 min, rinsed again with DDI water, and finally dried under nitrogen gas.

Surfaces of the clean glass chips were next silanized by immersion in a 1% MPTS (3-mercaptopropyl trimethoxysilane), 95% methanol, and 4% 1 mM acetic acid solution at room temperature for 30 min. The chips were then sonicated (300-W Vibracell probe sonicator, Sonic & Material Inc.) in a 95% ethanol: 5% water solution for 2 min, and dried under nitrogen gas.

Ag nanoparticles were covalently attached to the thiolated glass slides by immersing the silanized chips in a 10 mM $AgNO_3$ solution in dimethylformamide (DMF) for 1 h. The Ag nanoparticle coated glass slides were then washed by sonication in a 95% ethanol: 5% water solution for 4 min. They were finally dried under nitrogen gas prior to their storage under ambient conditions in the laboratory.

DNA probe array printing

DNA probes were printed using a Virtek Chip Writer Pro (Virtek Vision Inc., Ontario, Canada) microarrayer and an SMP2XB pin (Arrayit Corporation, ~1 nL spot volume, ~120 μm spot diameter). The DNA probe solution used for printing consisted of 900 nM DNA probe and 180 nM MP (mercaptopropanol) in buffered saline containing 10% glycerol (250 mM NaCl, 10 mM cacodylic acid, and 0.25 mM EDTA (ethylenediaminetetraacetic acid), pH = 7). DNA self-assembly on the nanostructured Ag substrate surface was accomplished by allowing the spots to immobilize for 1 h at 75% humidity in the dark.

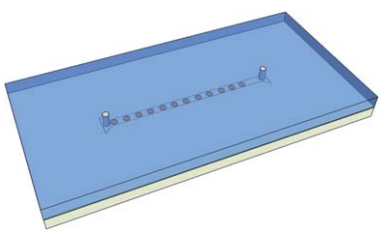

Fig. 2 Schematic of the simple microfluidic device employed in this study. The PDMS microchannel is covalently bonded to an Ag nanoparticle surface carrying an array of DNA hairpin probe spots (represented by circles). Spot size, number of spots, and channel dimensions are not drawn to scale.

Next, non-specifically absorbed DNA hairpin probes were removed by immersing the substrates in boiling DDI water for 30 s. Substrates were then air dried and left in the dark for 45 min. Once the probe spots were immobilized on the substrate surfaces, the substrates were covalently bound to the channel-embedded PDMS replicates as described below. As a final step, hairpin reformation was promoted by adding 1 μl of buffered saline (500 mM NaCl, 20 mM cacodylic acid, and 0.5 mM EDTA, pH = 7) into the channel for 45 min (room temperature, in the dark).

Probe and target DNA sequence

Initial studies in this report employed a previously described DNA probe (5′- TCG TTA GTG TTA GGA AAA AAT CAA ACA CTC GCG A-3′, designed based on gene-folding analysis of the *Bacillus anthracis* pag gene[18]). The target cDNA has a sequence of 5′- TCG CGA GTG TTT GAT TTT TTC CTA ACA CTA ACG A-3′. The multiplex study employed probes designed to be specific for uropathogenic *E. coli* (Eco3a: 5′-CTG AGC CTC ACC AAC GAA GAA CTG GCT CAG-3′) and *Enterobacter cloacae* (Enterbact3a: 5′-GCG GCT TAA CAC TAA CTC GTT ATC CGC-3′). The target cDNAs have sequences of (1, Eco3a) 5′-CTG AGC CAG TTC TTC GTT GGT GAG GCT CAG-3′and (2, Enterbact3a) 5′-GCG GAT AAC GAG TTA GTG TTA AGC CGC-3′, respectively. Further details of their design may be found in Supplementary Information.† All probes were purchased from Midland Certified, Inc., and bear a 3′-tetramethyl rhodamine (TMR) fluorophore (Ab_{max}, 559 nm; Em_{max}, 583 nm) and a 5′ trityl-thiol.

Microfluidic device fabrication

The microchannel used in this study is 2 cm in length, 1 mm in width, and 50 μm in height, connected to two isosceles trapezoid fluidic reservoirs (top base: 1 mm, bottom base: 3.75 mm, and height: 1.25 mm) at both ends. Total fluid volume of our channel is 1 μl. The channel-embedded PDMS replicates were fabricated by casting 20 grams of the PDMS elastomer mixture (at a prepolymer: curing agent ratio of 10 : 1 (w/w), Sylgard 184 kit, Dow Corning, Midland, MI) over a SU-8 photoresist mask. The photoresist mask has an inverse feature of the microchannels, and was patterned using standard soft lithography at Stanford Microfluidics Foundry (Stanford, CA).

After initial casting, the overlaying PDMS mixture was cured at 110 °C for 2 h, and the cured channel-embedded PDMS replicates were peeled away from the mask using forceps. Inlet and outlet of the channels were created by punching holes at both reservoirs using blunt-end needles (20G × ½″ stainless steel, Small Parts, Inc, FL).

The channel-embedded PDMS replicates were next bound to individual probe-immobilized Ag substrates. One standard approach to creating a covalent O–Si–O bond between PDMS and a glass substrate is through oxygen plasma treatment. As PDMS is composed of repeating $–OSi(CH_3)_2–$ chemical units, these can be converted to silanol (OH–Si) upon oxygen plasma exposure. These rapidly react with analogous groups on the glass surface.[20] Thus, after PDMS replicates had been cured and punched, we treated the surface with UV-ozone (Bioforce Nanosciences, Inc, model UV-TC.110) with the feature sides

facing up for 3 min. The UV-ozone treated-PDMS replicates were next placed in immediate contact with Ag substrates. Finally, the assembled PDMS replicate/Ag substrate complexes were heated in an oven at 110 °C for 10 min prior to storage. After channel assembly, inlet and outlet tubing (polyethylene, I.D. 0.55 mm, O.D. 0.965 mm) was connected to the channel reservoirs *via* blunt-end needles (22G × 1/2″ stainless steel, Small Parts, Inc., FL). Inlet tubing was connected to a 1 ml syringe (Norm-Ject®) mounted on a syringe pump (model: NE-1000 Multi-Phase™, New Era Pump Systems Inc., NY). Outlet tubing was connected to a waste reservoir. Target solutions with different concentrations in buffered saline (500 mM NaCl, 20 mM cacodylic acid, and 0.5 mM EDTA, pH = 7) were delivered into the channel *via* a syringe pump at a flow rate of 0.5 μl min^{-1}.

Data acquisition

Fluorescence measurements were performed using an Olympus BX-60 fluorescence microscope equipped with a thermoelectrically (TE) cooled charge coupled device (CCD). Samples were excited with incident light from a Hg lamp (100-W), which was filtered with an excitation bandpass filter (531 ± 20 nm), reflected by a dichroic mirror, and guided through a 10X objective lens. The emitted light was collected by the CCD after being directed from the sample, through the objective, the dichroic mirror, and an emission bandpass filter (593 ± 20 nm). Fluorescence images were analyzed using Image J software.[21]

Results and discussion

Unlike traditional microfluidic devices, where the channel-embedded PDMS blocks are placed in immediate contact with the glass substrate base, our device design prevents direct contact between the PDMS replicates and the glass slides since the base is covered with Ag nanoparticles. Thus, it was not clear *a priori* whether bonding could be achieved between the microfluidic channel and the sensor substrate. However, preliminary trials indicated that covalent bonding between PDMS replicates and Ag nanoparticle substrates was readily achievable using the protocol described above. The assembled microfluidic devices showed no evidence of channel collapsing. Furthermore, flow rates of up to 30 μl min^{-1} (with a duration up to 30 min) were readily sustained without any evidence of channel leakage. Fluidic flow velocities higher than 30 μl min^{-1} were not tested, as this fluidic flow was more than sufficient for our study. To our knowledge, this is the first demonstration of direct covalent bonding between PDMS blocks and metal nanoparticle-coated glass slides. As an alternative, Ag substrates could be prepared by patterning MP (mercaptopropanol) and Ag nanoparticles sequentially on the glass (merely patterning MP on the glass followed by non-selective Ag nanoparticle deposition will result in non-specific absorption of Ag nanoparticles on glass surface[22]). Next, the channel that is embedded in the PDMS block could then be aligned and bound to the patterned Ag nanoparticle surface with the help of an aligner. While this alternative process would be effective, it is clearly less efficient from a manufacturing standpoint due to the additional step of chemical patterning and or the use of the aligner.

How do the PDMS replicates form covalent bonds with the nanostructured Ag substrate? We hypothesized that covalent bonds formed between the bare glass space remaining between individual Ag nanoparticles and the PDMS surfaces. To verify this hypothesis, we attempted to bond PDMS replicates with continuous planar Au films using the same assembly method (UV-Ozone PDMS block followed by 110 °C treatment) as a control. Consistent with our hypothesis, we found that the PDMS replicates could be easily peeled away from the continuous Au surface with a pair of forceps, whereas the PDMS replicates stayed firmly attached to the nanostructured Ag substrate and could not be separated from each other without disrupting the PDMS.

After successfully addressing the challenge of assembling a leakage-free device, we next examined the utility of this microfluidic system for arrayed DNA detection. As opposed to previous studies in which the entire substrate surface was functionalized with hairpin probes, here we spotted different probe sequences on the substrate surface using a microarrayer. This approach not only provides the potential for multiplex detection, but also dramatically reduces reagent consumption. Prior to attempting multiplex detection, we first evaluated the impact of the microfluidic environment on a single probe-target pair. In this study, arrays of the *Bacillus anthracis* probe (2 columns, each column consisted of 10 probe spots) were first printed on the substrate surface and the substrate was next integrated with a channel-embedded PDMS replicate using the assembly protocols described in the experimental section. Using a standard fluorescence microscope for imaging, we were able to observe 4 spots within one fluorescence image under 10X objective magnification, and 8 spots under 4X objective magnification (Figure S1). These spots are approximately circular with a diameter of ~90 μm. By arraying spots in columns, we were able to incorporate two columns of spots into a single channel. One could further decrease the inter-spot distance to accommodate more DNA probe spots into the channel and hence increase the multiplex capability of the device. Exposure of a solution containing synthetic target to these probe-immobilized channels confirmed the device's ability to support DNA detection in an array format as evidenced by clear increases in fluorescence (Fig. 3).

To evaluate the potential utility of the device for real-time quantitative analysis, we challenged the probe-immobilized microchannels with target solutions containing different concentrations (0.125, 0.5, 2.5, and 25 μM). Target solutions were delivered into the microfluidic channels at a flow velocity of

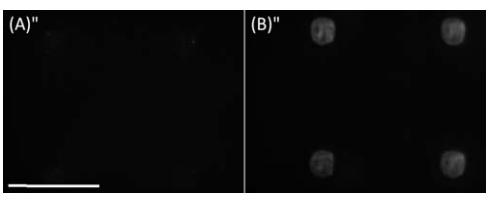

Fig. 3 Fluorescence microarray images showing the signals from four identical *Bacillus anthracis* probe spots on the channel floor (A) before and (B) after exposure to a 2.5 μM target solution that was introduced into the channel at a velocity of 0.5 μl min^{-1} for 30 min. Scale bar: 250 μm. CCD exposure time: 10 s.

0.5 μl min^{-1}, and fluorescence responses from the probe spots were recorded at time points of 0, 1, 2, 3, 4, 5, 6, 7, 8, 9, 10, 15, 20, 25, and 30 min during a continuous target fluid flow. Fluorescence intensity changes were obtained by subtracting the signals at each time point from the fluorescence intensity at 0 min, ($I_{time} - I_0$). As shown in Fig. 4, the fluorescence signal increased as a function of target delivery time, except for the control (no target) group. Detection time as low as ~6 min, corresponding to only 3 μl of the target solution, was sufficient to discern a signal difference between each group. No significant difference was observed between the 2.5 μM and the 25 μM group, suggesting that a 2.5 μM target concentration was sufficient to saturate the probe molecules on the substrate surfaces. The errors observed in each data point primarily resulted from chip-to-chip variations, as opposed to intra chip (inter spots on the same substrate) variations. This variation is likely due to variability in the array printing process.

To demonstrate the capability of this microfluidic device to detect lower concentrations of target analytes, we next exposed sensors to 25 nM, 5 nM, 500 pM, and 0 M target solutions. Here, analyte solutions were delivered continuously at a speed of 0.5 μl min^{-1} for 2 h. Fluorescence images of the DNA probe spots on the microchannel floors were acquired at 5 min time intervals after target injection. As one would expect, longer delivery times were required for these low-concentration solutions (Fig. 5). However, the observed minimum detection time is significantly less than what was required in previous studies of non-fluidic systems. For example, overnight incubations were necessary in the non-flow format in order to generate a detection signal from 10 pM target solutions.[18] It is likely that detection time can be further reduced by increasing target delivering speed, thus allowing a more efficient target analyte transport to the reaction surfaces. This is supported by a time scale calculation, which shows that the diffusion time scale of a 30mer target DNA ($D = 90 \times 10^{-8}$ cm^2 s^{-1})[23] in a 50 μm tall microchannel (~28 s, $t_d = h^2 D^{-1}$) is more than 4 times smaller than the convection time scale in a 2 cm long channel with a flow velocity of 0.5 μl min^{-1} (120 s, Q/A (Q: volumetric flow rate, A: cross-sectional area of the channel)). Thus, a higher flow rate will accelerate target delivery to the reaction surfaces and concomitantly maximize the usage of target analyte.

Statistical analysis shows that the detection signals (at the 120 min time points) from different concentrated target solutions are all significantly different from the control group. In this

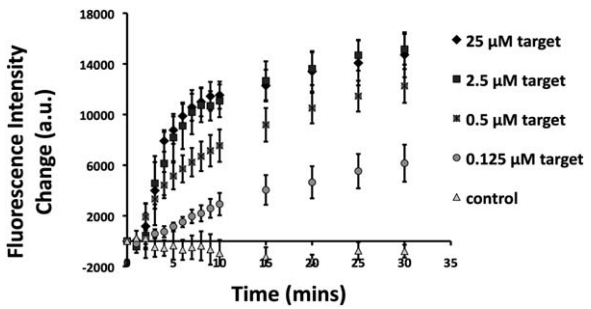

Fig. 4 Real-time fluorescence intensity changes as a function of different target concentrations. Data are presented as mean ± standard deviation. N = 3 (3 microfluidic channels). CCD exposure time: 10 s.

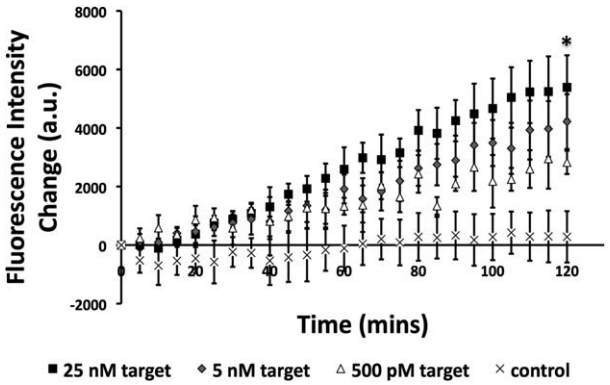

Fig. 5 Detection responses from 12 microfluidic channels upon introduction of target DNA solutions containing different concentrations (25 nM, 5 nM, 500 pM, and 0 M target). Data are presented as mean ± standard deviation. N = 3 (3 microfluidic channels). CCD exposure time: 10 s. Statistical analysis was performed using one-way ANOVA with *tukey post hoc* test, Matlab. N = 3 (3 channels). (*) Significant difference was found between any two groups.

unoptimized system, the limit of detection (LOD) is determined to be 500 pM, which is comparable with other label-free plasmonic DNA biosensors that require no sample enrichment.[24] We believe the LOD can be further reduced by increasing flow time and/or the target flow rate, as supported by the above calculations. In addition, significant difference was discerned between any two groups, suggesting this device can be employed for quantitative detection.

As discussed earlier, an ideal biosensor should exhibit multiplexing capability, as detecting multiple target DNA sequences can simultaneously increase sample throughput and also enable quantitative analyses of multiple targets in one example. Parallel detection is also tantamount to low reagent consumption and reduction in laborious procedures that are usually required in non-multiplex settings.

To demonstrate multiplex detection in our microfluidic device, probes containing different DNA sequences (Enterbact3a and Eco3a) were printed in two different rows on Ag substrates. A 500 nM target solution containing DNA complementary to the Enterbact3a probes was then flowed through the channel. The target DNA molecules were delivered to the microfluidic device at a flow rate of 0.5 μl min^{-1} for 30 min.

Fig. 6 shows the real-time fluorescence intensity change during a continuous fluid flow of a 500 nM Enterbact3a target solution in the microchannel. Fluorescence intensity change from the Enterbact3a probe spots was found to be ~6 fold higher (2232) than the fluorescence intensity from the Eco3a group (390) after 30 min target exposure time. A detection time of less than 5 min was sufficient to generate distinguishable signals from the negative control groups (Fig. 6).

Though there is minimal detection response from the Eco3a probe spots upon target introduction, the response did appear to be greater than the negative control, in which only buffer was applied to the system (Fig. 7). This subtle increase in detection response that was observed from the Eco3a probe spots could be due to non-specific interactions. Modifying the hybridization environment to more stringent conditions (higher temperature or lower salt concentration) could potentially reduce these

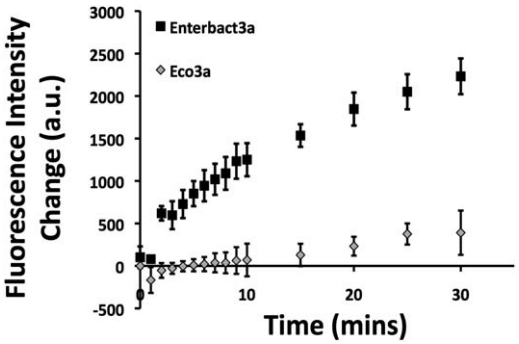

Fig. 6 Real-time fluorescence responses during a continuous target solution flow for a multiplex sensor. The 500 nM synthetic Enterbact3a target DNA solution was delivered to the device at a speed of 0.5 μl min^{-1} for 30 min. Data are presented as mean ± standard deviation. N = 3 (3 microfluidic channels). CCD exposure time: 10 s.

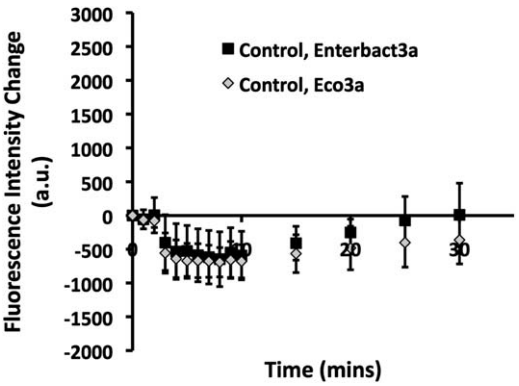

Fig. 7 Fluorescence intensity changes from 6 microfluidic channels upon introduction of buffer only into the device at a velocity of 0.5 μl min^{-1} for 30 min. Substrate surfaces were arrayed with Enterbact3a and Eco3a probes. Data are presented as mean ± standard deviation. N = 3 (3 microfluidic channels).

background signals. We also observed that in response to identical amounts of target DNA molecules, the detection responses obtained in this study was ~5 fold lower than the signal change obtained from the *Bacillus Anthracis* detection study. This difference could be due to subtle differences in the ability of the two probes to assemble on the Ag nanoparticle surface, or may result from differences in hybridization kinetics between the two target DNA sequences.

Conclusions

This report demonstrates a real-time and arrayable DNA biosensor in a microfluidic device using Ag nanoparticle-bound DNA hairpin probes. At a target flow rate of 0.5 μl min^{-1}, only 4 μl of 125 nM target solution was required to elicit a significant detection signal. Our subsequent efforts further established this device's capability for multiplex detection. While only 4–8 sample spots could be identified at once with our current imaging (under 10X and 4X objective magnification, respectively) and microarray setup, higher sample throughput can be achieved by decreasing inter-spot distance or through the use of a fluorescence scanner. These studies confirm the adaptability of the Ag nanoparticle-enabled DNA sensor to a microfluidic format, and suggest that further study of applications of this simple label-free (or "self labelled") detection system will be warranted.

Acknowledgements

HP thanks Amrita R. Yadav and Rashmi Sriram for assistance with the microarrayer.

References

1 P. Gascoyne, C. Mahidol, M. Ruchirawat, J. Satayavivad, P. Watcharasit and F. F. Becker, *Lab Chip*, 2002, **2**, 70.
2 E. L. Kwak, S. Digumarthy, A. Muzikansky, P. Ryan, U. J. Balis, R. G. Tompkins, D. A. Haber and M. Toner, *Nature*, 2007, **450**, 1235.
3 M. Bercovici, G. V. Kaigala, K. E. Mach, C. M. Han, J. C. Liao and J. G. Santiago, *Anal. Chem.*, 2011, **83**, 4110.
4 P. S. Waggoner, C. P. Tan and H. G. Craighead, *Sens. Actuators, B*, 2010, **150**, 550.
5 R. Peytavi, F. R. Raymond, D. Gagne, F. J. Picard, G. Jia, J. Zoval, M. Madou, K. Boissinot, M. Boissinot, L. Bissonnette, M. Ouellette and M. G. Bergeron, *Clin. Chem.*, 2005, **51**, 1836.
6 C. Zhang and D. Xing, *Nucleic Acids Res.*, 2007, **35**, 4223.
7 Y. Zhang and P. Ozdemir, *Anal. Chim. Acta*, 2009, **638**, 115.
8 F. B. Myers and L. P. Lee, *Lab Chip*, 2008, **8**, 2015.
9 C. D. Chin, V. Linder and S. K. Sia, *Lab Chip*, 2007, **7**, 41.
10 J. H. Sung, C. Kam and M. L. Shuler, *Lab Chip*, 2010, **10**, 446.
11 S.-W. Yeung, T. M.-H. Lee, H. Cai and I.-M. Hsing, *Nucleic Acids Res.*, 2006, **34**, e118.
12 A. Hirsch, C. Rivet, B. Zhang, M. L. Kemp and H. Lu, *Lab Chip*, 2009, **9**, 536.
13 J. Wang, D. Onoshima, M. Aki, Y. Okamoto, N. Kaji, M. Tokeshi and Y. Baba, *Anal. Chem.*, 2011, **83**, 3528.
14 J. Zhang, Y. Fu, M. H. Chowdhury and J. R. Lakowicz, *Nano Lett.*, 2007, **7**, 2101.
15 H. Du, M. D. Disney, B. L. Miller and T. D. Krauss, *J. Am. Chem. Soc.*, 2003, **125**, 4012.
16 C. M. Strohsahl, B. L. Miller and T. D. Krauss, *Nat. Protoc.*, 2007, **2**, 2105.
17 H. Du, C. M. Strohsahl, J. Camera, B. L. Miller and T. D. Krauss, *J. Am. Chem. Soc.*, 2005, **127**, 7932.
18 C. M. Strohsahl, T. D. Krauss and B. L. Miller, *Biosens. Bioelectron.*, 2007, **23**, 233.
19 H.-I. Peng, C. M. Strohsahl, K. E. Leach, T. D. Krauss and B. L. Miller, *ACS Nano*, 2009, **3**, 2265.
20 S. K. Sia and G. M. Whitesides, *Electrophoresis*, 2003, **24**, 3563.
21 M. D. Abramoff, P. J. Magelhaes and S. Ram, *Biophoton. Int*, 2004, **11**, 36.
22 I. Pastoriza-Santos, C. Serra-Rodriguez and L. M. Liz-Marzan, *J. Colloid Interface Sci.*, 2000, **221**, 236.
23 V. Chan, D. J. Graves and E. McKenzie, *Biophys. J.*, 1995, **69**, 2243.
24 H.-I. Peng and B. L. Miller, *Analyst*, 2011, **136**, 436.